Local heat flux and energy loss in a two-dimensional vibrated granular gas

Olaf Herbst,* Peter Müller, and Annette Zippelius
Institut für Theoretische Physik, Georg-August-Universität, D-37077 Göttingen, Germany
(Received 13 December 2004; revised manuscript received 14 June 2005; published 14 October 2005)

We performed event-driven simulations of a two-dimensional granular gas between two vibrating walls and directly measured the local heat flux and local energy dissipation in the stationary state. Describing the local heat flux as a function of the coordinate x in the direction perpendicular to the driving walls, we test a generalization of Fourier's law, $q(x)=-\kappa\nabla T(x)+\mu\nabla\rho(x)$, by relating the local heat flux to the local gradients of the temperature and density. This *ansatz* accounts for the fact that heat flux can also be generated by density gradients, not only by temperature gradients. Assuming the transport coefficients κ and μ to be independent of x, we check the validity of this assumption and test the generalized Fourier law in the simulations. Both κ and μ are determined for different system parameters, in particular, for a wide range of coefficients of restitution. We also compare our numerical results to existing hydrodynamic theories. Agreement is found for κ for very small inelasticities only, i.e., when the gradients are small. Beyond this region, κ and μ exhibit a striking nonmonotonic behavior. This may hint that hydrodynamics to Navier-Stokes order cannot be applied to moderately inelastic vibrated systems.

DOI: 10.1103/PhysRevE.72.041303 PACS number(s): 45.70.−n, 51.10.+y, 51.30.+i

Driven granular gases have attracted much attention in recent years [1–7]. This is partly because in these systems, energy loss in inelastic collisions is eventually balanced by energy input from the driving so that a stationary state can be attained. In physically realistic models, the driving usually acts at the boundaries of the system, e.g., in terms of shearing forces or vibrating walls. Thus, maintaining a stationary state requires a subtle and well-balanced mechanism to transfer energy from the system's boundaries to its interior. The local energy (or heat) flux and the local energy-dissipation rate are, therefore, at the heart of every hydrodynamic description [5,8–11] of the stationary state of driven granular gases.

Hydrodynamic approaches to granular media require the knowledge of constitutive relations for the pressure tensor, heat flux, and local energy loss in order to close the balance equations for mass, momentum, and energy. In a previous work, we presented the pressure tensor and found that a local constitutive relation holds while, in general, it is not universal [6]. Here, we focus on the remaining two constitutive relations.

Fourier's law states for elastic systems that the heat current is proportional to the local temperature gradient, the proportionality constant being the thermal conductivity κ [12]. For inelastic systems, there is an additional contribution to the heat current from density gradients [8]. The corresponding transport coefficient μ has no analog in elastic systems. Theoretical approaches start from the Boltzmann-Enskog equation to account for these effects. Jenkins and Richman [8] have used Grad's moment expansion to compute the heat flux for small inelasticity, whereas Dufty *et al.* [9] have pushed kinetic models using a *stosszahl ansatz* to simplify the collision operator. Molecular dynamics (MD) simulations have been performed by Soto *et al.* [13] to study μ for a granular gas on a vibrated plane in the dilute limit.

In this paper, we study the local heat flux and local energy-loss rate, as well as the transport coefficients κ and μ for a driven granular gas in two dimensions. We perform event-driven simulations of N identical inelastic smooth hard disks of diameter a and mass m which are confined to a rectangular box with edges of length L_x and L_y. Periodic boundary conditions are imposed in the y direction, and the gas is driven through the walls perpendicular to the x direction, see Fig. 1 for a typical snapshot. The left and right walls vibrate in an idealized sawtooth manner, characterized by the driving velocity $v_{\text{drive}}>0$: Upon a collision of a particle with the left or right wall at $x=\mp L_x/2$, the x component of its velocity changes according to $v_x'=-2v_x\pm v_{\text{drive}}$, see also Ref. [6]. Inelastic interparticle collisions are modeled using a constant coefficient of normal restitution $\alpha\in]0,1[$ according to $\hat{\mathbf{n}}\cdot\mathbf{v}_{12}'=-\alpha\hat{\mathbf{n}}\cdot\mathbf{v}_{12}$. Here, $\hat{\mathbf{n}}$ denotes the unit vector of the particles' relative center-of-mass positions, and $\mathbf{v}_{12}$, resp. $\mathbf{v}_{12}'$ are the precollisional, respectively, postcollisional relative center-of-mass velocities.

A simple estimate in Ref. [6] yields for the spatially averaged granular temperature $T_0=N^{-1}\Sigma_{i=1}^{N}m\mathbf{v}_i^2/2$ in the stationary state

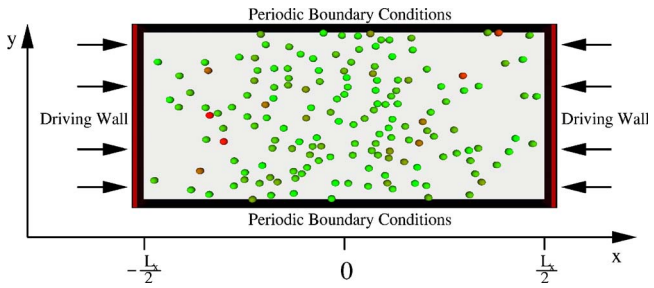

FIG. 1. (Color online) Model of N disks driven in the x direction with periodic boundary conditions in the y direction.

*Electronic address: olaf.herbst@gmx.net

 ©2005 The American Physical Society

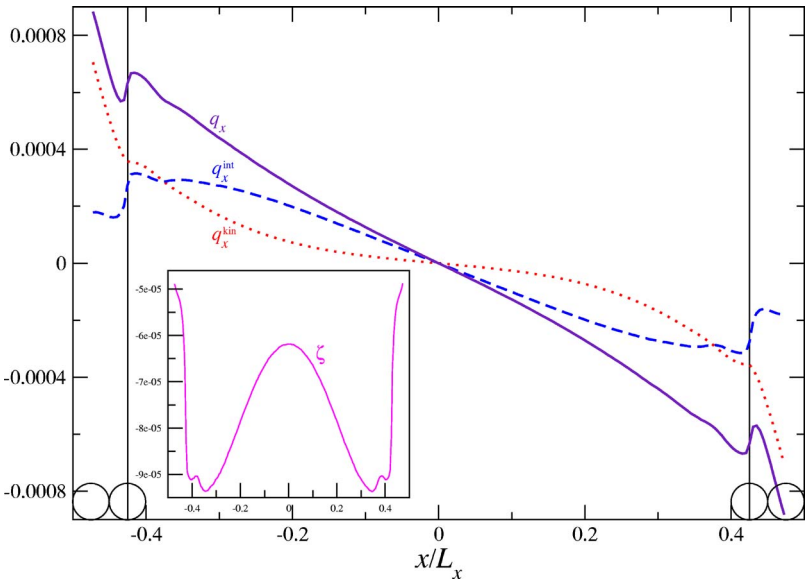

FIG. 2. (Color online) Heat flux in the x direction q_x (in dimensionless units) for a system of $N=256$ particles with coefficient of restitution $\alpha=0.9$ in a box of size $L_x=20$ and $L_y=25$, corresponding to a total area fraction of $\phi_0=0.4$. The dotted line shows the kinetic part q_x^{kin}; the dashed line is the collisional part q_x^{int}; and the full line represents the total heat flux q_x. The inset displays the local energy-loss rate ζ.

$$\frac{T_0}{mv_{\mathrm{drive}}^2/\varepsilon^2} \approx \left(\frac{2}{\pi}\right)^3 \psi^{-2}(1+\sqrt{1+(\pi/2)^2\varepsilon\psi})^2. \tag{1}$$

Here $\varepsilon := 1-\alpha^2$ and $\psi := \sqrt{2}\chi\lambda$ are dimensionless parameters. The latter involves the pair correlation at contact χ of the corresponding elastic system and the line density $\lambda := N/L_y$.

In the following discussion of heat flux and dissipation, we will, *inter alia*, be interested in a *scaling limit* $\varepsilon \downarrow 0$ towards an elastic system. In order to prevent the system from heating up indefinitely when switching off dissipation, we also need to scale the driving velocity $v_{\mathrm{drive}} =: \varepsilon v_0$, where v_0 is fixed. Hence, the driving vanishes in the elastic scaling limit, and the spatially averaged temperature reaches a finite value, approximately given by $T_0 \approx 16/\pi^3(\chi\lambda)^{-2}mv_0^2$ according to Eq. (1).

Locally, the translational energy changes due to collisions as well as due to free streaming of the particles in between collisions. The latter gives rise to a kinetic contribution to the heat current $\mathbf{q}^{\mathrm{kin}}$, whereas the collisions are responsible for the energy loss ζ as well as for the collisional contribution to the heat current $\mathbf{q}^{\mathrm{int}}$. For vanishing macroscopic velocity, the energy balance equation is usually formulated as [8,9]

$$\rho(\mathbf{r},t)\frac{\partial}{\partial t}T(\mathbf{r},t) = -\boldsymbol{\nabla}\cdot\mathbf{q}(\mathbf{r},t) + \zeta(\mathbf{r},t) \tag{2}$$

for the hydrodynamic fields of density ρ, temperature T, total heat current $\mathbf{q}=\mathbf{q}^{\mathrm{kin}}+\mathbf{q}^{\mathrm{int}}$, and local energy dissipation rate ζ.

To compare our simulations to the hydrodynamic theory, we need to introduce a coarse graining function $\Phi(\mathbf{r})$ [14], which is nonzero in a small area centered at $\mathbf{r}$ only. We require, of course, $\int d\mathbf{r}\Phi(\mathbf{r})=1$. In the absence of a velocity field, the coarse grained kinetic heat current is defined by

$$\mathbf{q}^{\mathrm{kin}}(\mathbf{r},t) = \sum_{i=1}^{N} \frac{m\mathbf{v}_i^2}{2}\mathbf{v}_i\Phi(\mathbf{r}-\mathbf{r}_i). \tag{3}$$

The coarse grained density $\rho(\mathbf{r})$ and temperature $T(\mathbf{r})$ are defined analogously.

The change of energy during a binary collision in a small time interval Δt can be decomposed into a source term and a divergence of a flux. The coarse grained energy dissipation rate $\zeta(\mathbf{r},t)$ can be calculated analogous to [14] and is given by

$$\zeta(\mathbf{r},t) := \frac{1}{2\Delta t}\sum_{i,j}{}' (\Delta E_{i|j} + \Delta E_{j|i})\Phi(\mathbf{r}-\mathbf{r}_i) \tag{4}$$

in terms of the change of energy $\Delta E_{i|j}$ of particle i due to a collision with particle j in the time interval $[t,t+\Delta t]$. The prime at the summation sign restricts i and j to those particles colliding in Δt. The energy dissipation rate trivially vanishes in the elastic case, when $\Delta E_{i|j}=-\Delta E_{j|i}$. Similarly, the collisional contribution to the heat current is given by

$$\mathbf{q}^{\mathrm{int}}(\mathbf{r},t) := \frac{1}{4\Delta t}\sum_{i,j}{}' (\Delta E_{i|j} - \Delta E_{j|i})\mathbf{r}_{ij}\int_0^1 \Phi(\mathbf{r}-\mathbf{r}_i+s\mathbf{r}_{ij})ds, \tag{5}$$

where $\mathbf{r}_{ij}=\mathbf{r}_i-\mathbf{r}_j$. In our simulations we have never found any significant variations of the long time averages of the hydrodynamic fields in the y direction parallel to the driving walls. Hence, we coarse grain our system by subdividing the box into strips of width Δx.

In the following, we report numerical results on the stationary state only. For more details of the simulations, such as initialization or relaxation toward the stationary state, the reader is referred to Ref. [6]. For dimensional reasons, the driving velocity v_0 sets the time and energy scale and is chosen to be 1. Likewise, the particle mass and diameter set the mass and length scales.

We first present data for the heat-flux profile in Fig. 2 for a system of global area fraction $\phi_0 := N\pi/(4L_xL_y)=0.4$ and coefficient of normal restitution $\alpha=0.9$. More precisely, the figure displays the x component of the heat flux and its kinetic and collisional part as a function of the normalized position x/L_x. The inset shows the local energy-loss rate and will be discussed below. The heat flux is antisymmetric about

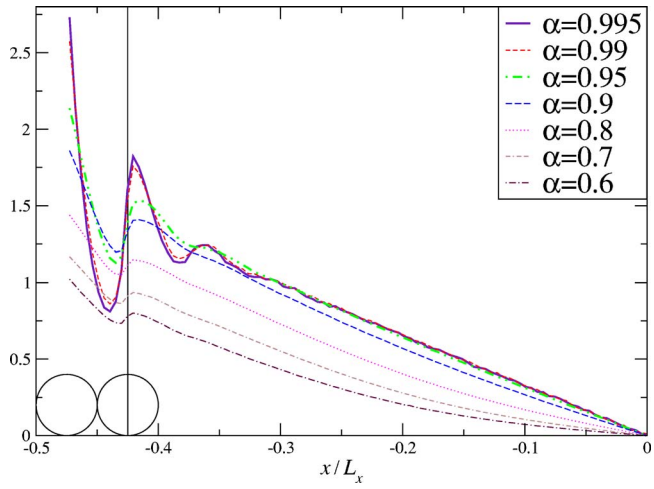

FIG. 3. (Color online) Rescaled (dimensionless) heat flux q_x/ε for a wide range of coefficients of restitution $0.6 \leqslant \alpha \leqslant 0.995$ for otherwise fixed systems ($L_x=20$, $\phi_0=0.4$).

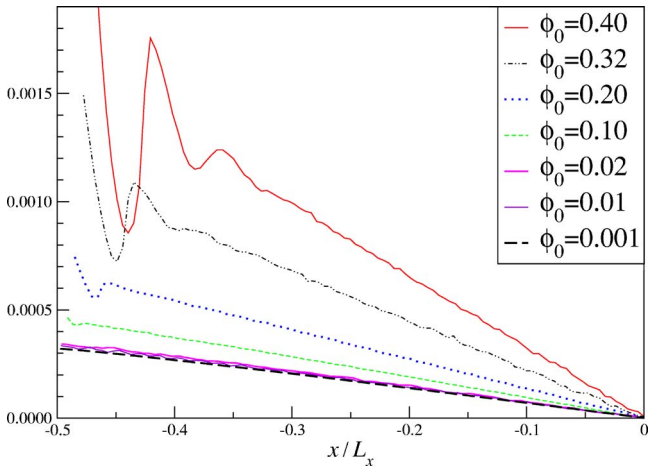

FIG. 4. (Color online) Rescaled (dimensionless) heat flux $L_x q_x$ for a wide range of box edges (area fraction $0.001 \leqslant \phi_0 \leqslant 0.4$ at fixed line density $N/L_y=10.24$ and fixed coefficient of restitution $\alpha=0.99$. This graph looks almost the same for all $\alpha \geqslant 0.9$.

the middle of the system as expected. We clearly see that its collisional part, Eq. (5), which is represented by the dashed line cannot be neglected. It is of the same order of magnitude as the kinetic contribution—depicted by the dotted line and corresponding to Eq. (3). For lower density systems, the collisional contribution becomes less important but still it is not negligible for global area fractions even as low as $\phi_0=0.1$. This is not surprising since the collisional part is known to be important in elastic hard sphere systems, but to our knowledge it has not been directly measured in systems of inelastic hard spheres before. Interestingly, both the kinetic and the collisional contribution are nonlinear in the position x. However, the combination of both, resulting in the total heat flux, is almost linear throughout the system.

Now we turn to the dependence of the heat flux on the coefficient of restitution α in the elastic scaling limit. We recall that the driving strength has been adjusted such that the granular gas attains a finite temperature as $\varepsilon \to 0$. The heat flux is proportional to the temperature per time and, hence, is expected to scale like $T_0 v_{\text{drive}} \sim \varepsilon$ [cf. Eq. (1)]. This argument is checked by plotting q_x/ε for different coefficients of restitution in Fig. 3. The collapse of different data sets is excellent for almost elastic systems ($\varepsilon \ll 1$, i.e., $\alpha \gtrsim 0.95$). For higher inelasticities, this scaling no longer holds.

In Fig. 4, we show the rescaled heat flux $L_x q_x$ for a fixed coefficient of restitution $\alpha=0.99$ and various system sizes L_x. It has been shown [6] that the scale for temperature inhomogeneities is set by L_x, so that we expect the heat flux to scale like L_x^{-1}, if plotted versus x/L_x. For dilute systems ($\phi_0 \lesssim 1\%$), we get a decent data collapse. For higher densities, this scaling captures the correct order of magnitude only.

It is a characteristic feature of hydrodynamics of inelastically colliding particles that a heat current can be generated not only by a nonuniform temperature, but also by density inhomogeneities. If the spatial variations of temperature or density are restricted to long wavelengths, one would expect a gradient expansion to hold. The simplest constitutive equation for the heat flux is thus a straightforward generalization of Fourier's law, as discussed in the literature (cf. [12]). Chapman-Enskog expansions of both the Boltzmann and the Boltzmann-Enskog equations predict that the heat flux of an inelastic system is given

$$q_x(x) = -\kappa \frac{d}{dx} T(x) + \mu \frac{d}{dx} \rho(x), \tag{6}$$

where κ is the heat conductivity and μ is a new transport coefficient that has no analog for elastic systems [8,9].

To check the validity of Eq. (6), we estimate the transport coefficients from our data by assuming that both κ and μ do not depend on the position x, i.e., we assume them to be constant throughout the box. It is then straightforward to extract these transport coefficients from a fit of our data to the above expression (6). In Fig. 5, we show both transport coefficients κ and μ/ε. Both are nonmonotonic in α. In the elastic limit, we find that κ tends to a nonzero constant, while $\mu \propto \varepsilon$. At moderately high densities, the fit of the heat flux to Eq. (6) with constant fit parameters κ and μ is very good for all investigated α, e.g., for $\alpha=0.9$ or $\alpha=0.99$, it matches the heat flux from our simulations very well as can be seen in the top row of Fig. 6 (bold dotted lines lie on top of full [indigo] lines). Note, however, that our fitting procedure becomes increasingly difficult as $\alpha \to 1$ because the temperature gradient becomes proportional to the density gradient. Consequently, it is not possible for $\alpha \to 1$ to determine two parameters from the fit unambiguously.

We conclude that the generalized Fourier law holds as a constitutive relation for the heat flux. For lower densities and higher inelasticities, the gradients increase and the fit becomes worse implying a failure of the generalized Fourier law. Notice that the original Fourier law $q=-\kappa \nabla T$ does not hold whereas its generalization does (see Fig. 6).

Both transport coefficients have been computed within kinetic theory for small inelasticities by Jenkins and Richman [8], who find for the thermal conductivity

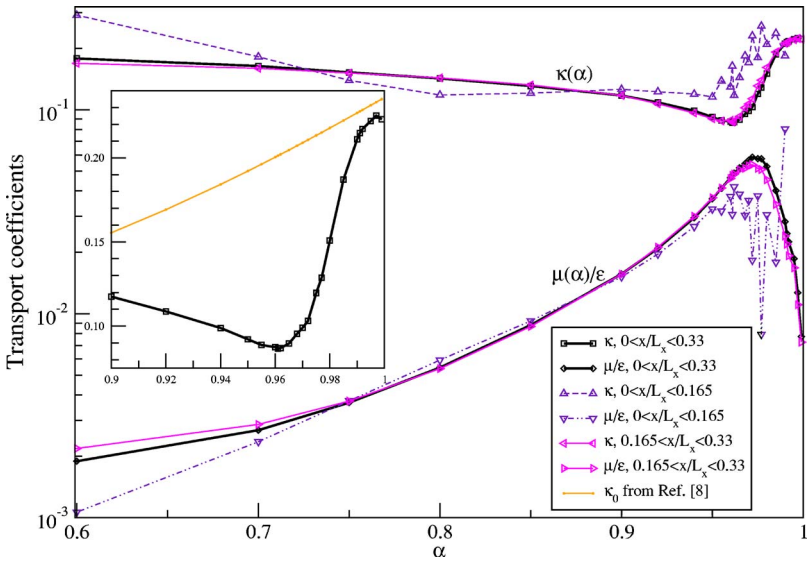

FIG. 5. (Color online) Transport coefficients κ and μ as functions of the coefficient of restitution α for systems of size $L_x=20$ and line density $N/L_y=10.24(\phi_0=0.4)$.

$$\kappa=\left[\frac{2+3\phi\chi r^2(4r-3)}{r\chi(17-15r)}(2+3\phi\chi r)+\frac{8\phi^2\chi r}{\pi}\right]\sqrt{\frac{T}{\pi}}, \quad (7)$$

where $r:=(1+\alpha)/2$. We use the Henderson approximation [15] for the pair correlation at contact χ, which is a function of the area fraction only. Inserting the local temperature $T(x)$ and local area fraction $\phi(x)$ from our simulations into (7), we obtain a spatially dependent transport coefficient $\kappa_{\mathrm{loc}}(x)$ and, from a corresponding equation in [8], $\mu_{\mathrm{loc}}(x)$. The resulting heat flux from Eq. (6) is shown in Figs. 6(a) and 6(b) (dashed [green] lines) and found to agree very well with the simulations for $\alpha\geqslant 0.99$. The agreement is reasonable even up to $\alpha\sim 0.96$. For larger inelasticities, the constitutive relation from Ref. [8] captures the correct order of magnitude, but overestimates the curvature of $q_x(x)$ [see Fig. 6(b)].

Alternatively, we can use the global or mean temperature T_0 and area fraction ϕ_0 to evaluate Eq. (7) and the respective equation from Ref. [8] for μ. In the inset of Fig. 5, we compare this κ_0 to the thermal conductivity κ obtained from fitting our simulations to Eq. (6). The agreement is reasonable as long as $\alpha\geqslant 0.99$. However, for inelasticities between $\alpha=0.9$ and $\alpha=0.99$ the heat conductivity κ from our simulations deviates strongly from the prediction of Ref. [8]. As to μ_0 (not shown), the deviations to μ are even stronger. This failure around $\alpha=0.95$ coincides with strongly increasing gradients which may hint that the hydrodynamics to first order in the gradients (Navier-Stokes order) is no longer valid. Our results also deviate strongly from the ones obtained in Ref. [13], most notably they find μ to be negative. Note, however, that in those simulations, the density is low and the density gradients are imposed by gravity. In our simulations, the density is much higher and tends to accumulate in the middle of the sample, away from the driving walls. The heat flux is directed from the walls to the center of the system and, hence, follows the gradient of the density. In a system without gravity, this seems physically plausible: regions of high density cool more efficiently due to an increased number of collisions and, hence, heat flows in.

The difference between $\kappa_{\mathrm{loc}}(x)$ and κ_0 is only a few percent for $\alpha\geqslant 0.99$. The difference in the corresponding heat fluxes is even less, because the strongest inhomogeneities in the transport coefficients occur in the middle of the sample where the gradients of temperature and density vanish. To demonstrate this, in the top row of Fig. 6, we also show the heat flux computed using *constant* transport coefficients κ_0 and μ_0 (i.e., inserting constant values into Eq. (7), dotted [red] lines). The fluctuations of the transport coefficients with the position x increase with increasing inelasticity, e.g., for $\alpha=0.9$, we find $\kappa_{\mathrm{loc}}(0)/\kappa_0\approx 1.5$.

To estimate the degree of inhomogeneity, we have divided the box into an inner and an outer part and fitted the heat current using data from either half of the box only. The scattering of the data from the inner and outer part is shown in Fig. 5 and provides a rough measure for the effects of inhomogeneous transport. The results for the outer half are almost identical to the ones for the full system. This is also true for the inner part except for the weakly inelastic systems for which the absolute value of the heat flux in the middle of the sample is so small that statistical fluctuations dominate.

The local energy loss, as defined in Eq. (4), is shown in the inset of Fig. 2 and in the bottom row of Fig. 6. Again, for $\alpha>0.99$ the agreement with the predicted $\zeta=-16\varepsilon\phi^2\chi(T/\pi)^{3/2}$ from [8] is very good in the bulk part of the sample. The large fluctuations close to the driving wall are due to the pair correlation function that enters the constitutive equation for the energy loss as well as the one for the heat flux. At higher inelasticities, deviations are clearly visible in the bulk, too. For very dilute quasi-elastic systems ($\phi_0\leqslant 0.1, \alpha\geqslant 0.95$), the dissipation is highest in the middle of the sample. For denser and/or more inelastic systems, we find the absolute value of ζ (the dissipation) to be greatest in an intermediate region $x\sim\pm 0.3L_x$. Even though the density is largest in the middle of the sample, energy dissipation is not very pronounced there because the mean kinetic energy is already comparatively small. Integrated over any part of the box, the local energy loss has to fulfill the conservation law $q_x(a)-q_x(b)=\int_a^b\zeta(x)dx$, where $-L_x/2\leqslant a\leqslant b\leqslant L_x/2$. We have checked it only for the case $-a=b=L_x/2$ in the simulations, which required careful measurements of the heat flux at the boundaries.

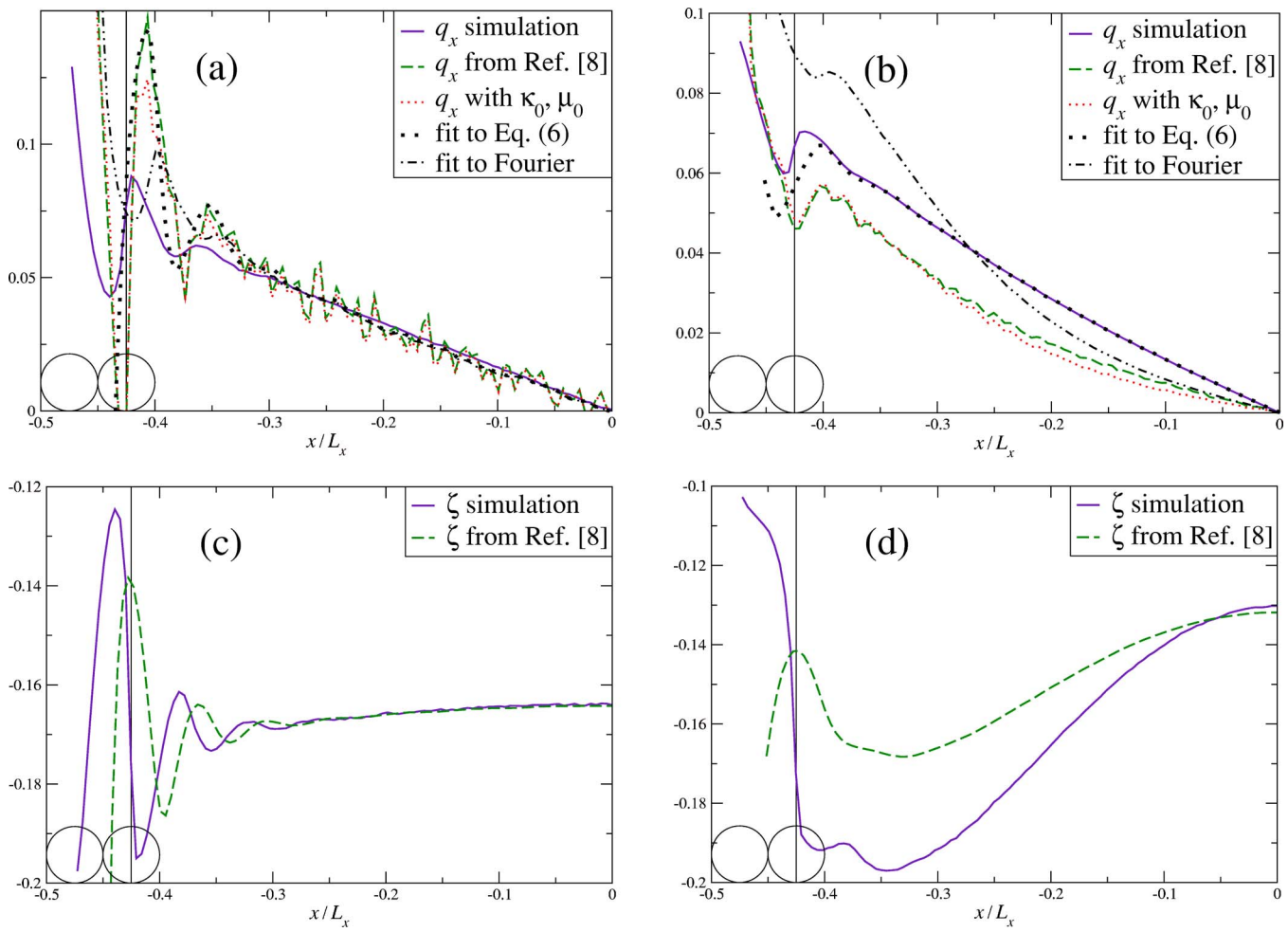

FIG. 6. (Color online) Comparison of heat flux (top row) and local energy loss (bottom row) for coefficients of restitution α=0.99 (left column) and α=0.9 (right column). The heat flux from our simulations is very well captured by Eq. (6) as the fit (bold dotted lines) confirms. For quasi-elastic systems, the constitutive relation for the heat flux as well as for the local energy loss calculated in Ref. [8] (dashed [green] lines) agrees well with our simulations. For higher inelasticities, the agreement is only qualitative. The dotted [red] lines show the same as the dashed [green] lines but with constant transport coefficients from Ref. [8]. The dashed-dotted lines show a fit to Fourier's law of heat conductivity.

In this paper, we have discussed the heat current in a granular gas driven by vibrating walls. We have measured the collisional contribution to the heat current and have shown that it cannot be neglected, not even in low density systems. We have extracted both transport coefficients of the heat flux for a wide range of inelasticities $0.6 \leqslant \alpha \leqslant 0.995$ and area fractions $0.01 \leqslant \phi_0 \leqslant 0.4$. The elastic limit has been studied in detail. It is reached by scaling the driving velocity with ε, so that the temperature tends to a finite value as $\alpha \to 1$.

Assuming the transport coefficients to be constant, we observed a nonmonotonic behavior: The thermal conductivity κ first decreases with increasing ε, goes through a minimum around $\alpha \approx 0.96$, and then increases again. The transport coefficient μ/ε first increases with ε, goes through a maximum at $\alpha \approx 0.96$, and then decreases again. Furthermore, a rough estimate of the fluctuations of the transport coefficients with spatial position in the box has been given. These effects are expected to be strong for moderately inelastic systems which are characterized by nonuniform density and temperature.

Comparing our data to theoretical work in two dimensions [8], we found good agreement for $\alpha \geqslant 0.99$. For stronger inelasticities, the temperature and density gradients increase and the theoretical predictions fail. This may imply that Navier-Stokes order hydrodynamics is not sufficient for describing moderately inelastic steady-state vibrated systems. Clearly, this point needs further investigation.

We thank Hans Vollmayr for pointing out to us the importance of the elastic limit and Isaac Goldhirsch for suggesting to investigate the heat flux. O.H. thanks Javier Brey, James Dufty, James Jenkins, and Christine Menzel for discussions. We acknowledge financial support by the DFG through SFB 602, as well as Grant Nos. Zi 209/6-1 and Mu 1056/2-1. This research was also supported in part by the National Science Foundation under Grant No. PHY99-0794.

[1] T. P. C. van Noije and M. H. Ernst, Granular Matter **1**, 57 (1998).
[2] C. Bizon, M. D. Shattuck, J. B. Swift, and H. L. Swinney, Phys. Rev. E **60**, 4340 (1999).
[3] R. Cafiero, S. Luding, and H. J. Herrmann, Phys. Rev. Lett. **84**, 6014 (2000).
[4] D. L. Blair and A. Kudrolli, Phys. Rev. E **67**, 041301 (2003).
[5] H. Hayakawa, Phys. Rev. E **68**, 031304 (2003).
[6] O. Herbst, P. Müller, M. Otto, and A. Zippelius, Phys. Rev. E **70**, 051313 (2004).
[7] M. Bose and V. Kumaran, Phys. Rev. E **69**, 061301 (2004).
[8] J. T. Jenkins and M. W. Richman, Phys. Fluids **28**, 3485 (1985).
[9] J. W. Dufty, J. J. Brey, and A. Santos, Physica A **240**, 212 (1997).
[10] N. Sela and I. Goldhirsch, J. Fluid Mech. **361**, 41 (1998).
[11] J. T. Jenkins and C. Zhang, Phys. Fluids **14**, 1228 (2002).
[12] S. Chapman and T. G. Cowling, *The Mathematical Theory of Nonuniform Gases* (Cambridge University Press, London, 1970).
[13] R. Soto, M. Mareschal, and D. Risso, Phys. Rev. Lett. **83**, 5003 (1999).
[14] B. J. Glasser and I. Goldhirsch, Phys. Fluids **13**, 407 (2001).
[15] D. Henderson, Mol. Phys. **30**, 971 (1975).